A.J. Hanson and D.J. Perreault, "Modeling the Magnetic Behavior of N-Winding Components," *IEEE Power Electronics Magazine*, vol. 7, no. 1, pp. 35-45, March 2020.

Modeling Magnetics

Introduction

In 2015, this magazine's cover portrayed gallium nitride (GaN) and silicon carbide (SiC) switching devices as super heroes, able to make "next-generation power electronics smaller, faster, and more efficient" in a single bound. And indeed, they are largely doing so, in conjunction with improved components and integrated circuits, better packaging and more sophisticated circuit design and control.

Despite this tremendous progress, magnetics remain an important bottleneck in power electronics. In some ways, this is inevitable. Magnetic components suffer from fundamental scaling laws that oppose miniaturization – a half-size magnetic component can process less than half of the power [1]. Other components have been more readily miniaturized by advances in materials, manufacturing, semiconductor devices, and operating frequencies. Meanwhile, magnetics remain stubbornly large and lossy – an even greater bottleneck than before. It is not uncommon in sophisticated, modern power converter designs to have approximately half of the volume and power losses arising from inductors and transformers. Visualizing this trend, our colleague has portrayed magnetics as a ball-and-chain locked around the ankles of the GaN and SiC super heroes (Fig. 1) [2].

Figure 1 - The potential for advances such as GaN and SiC to elevate system-level performance is often limited by the magnetic components.

Given this increasingly severe magnetic bottleneck, it is becoming imperative to make maximum use of magnetic capabilities, such as achieving multiple functions from a single component (e.g., using so-called "integrated" magnetics [3]). Magnetic components are relied upon to support multiple inputs/outputs (e.g. interfacing with a renewable energy source, a load, and a battery) [4]. They also allow the use of multiple voltage/current domains within a circuit to take advantage of good figure-of-merit switches at high frequency [5-6], advantageously spread out heat dissipation [7], or compress apparent impedance ranges [8]. In a great many of these cases, more functionality means more complicated magnetic components with more windings.

It is well known that magnetic components with multiple windings do not have simple behavior, and as switching frequencies increase and designs become more sophisticated, the importance of these more complex behaviors become increasingly central. In this article we review valuable techniques for modeling the magnetic behavior of inductors and (especially) multi-port components (e.g. transformers), highlighting each approach's advantages in component design, circuit application, and experimental characterization. Here we only model the behavior of magnetic coupling and energy storage within a component; there are many further aspects we do not treat here, such as capacitance modeling [9], winding loss modeling [10,11], and core loss modeling [12], though these can often be treated separately and appended to the models described here.

Modeling Magnetic Components

There are several ways to represent magnetic components, including:

1) Mathematical Representations
2) Necessary-and-Sufficient Circuit Representations
3) Physical Circuit Representations

For all three representations, single-winding structures (inductors) reduce to the same thing – a single inductance L represents the entire structure. The differences become more clear when a second winding is added to form a transformer. Here, the transformer can be represented by a set of coupled equations:

$$\begin{bmatrix} v_1 \\ v_2 \end{bmatrix} = \begin{bmatrix} L_{11} & L_{12} \\ L_{21} & L_{22} \end{bmatrix} \frac{d}{dt} \begin{bmatrix} i_1 \\ i_2 \end{bmatrix} \qquad (1)$$

where the inductance matrix comprises the *mathematical representation*. This representation fully captures the effect of inductive coupling among multiple electrical ports. By reciprocity [13], an inductance matrix must be symmetric, with $L_{mn} = L_{nm}$, which means there are $M(M+1)/2$ independent parameters in an *M*-winding structure. While independent, these parameters are nonetheless bound by the limitations of physics. For example, by conservation of energy, the inductance matrix must be positive semidefinite, yielding $L_{11} \geq 0, L_{22} \geq 0$, and $|L_{12}| \leq \sqrt{L_{11}L_{22}}$ in the two-port case.

While the inductance matrix is a useful mathematical description, it is not conducive to circuit analysis and design or to synthesis of magnetic components. To this end, the inductance matrix can also be represented by a "necessary-and-sufficient" equivalent circuit composed of inductors and ideal transformers. We call such models necessary and sufficient because they have the exact number of independent parameters needed to represent a magnetic structure. For a two-winding transformer, necessary-and-sufficient models can be constructed with each of the T model, the Pi model, and the Cantilever model (Fig. 2). These circuits will yield identical results to each other and to the mathematical representation.

Perhaps the most familiar of these is the T model, though it is more typically shown with inductor L_C reflected through the transformer to the secondary side (with an appropriate scaling of the inductance value). Defining the turns ratio $N_1/N_2 = N$, it is straightforward to show that the inductance matrix description can be related to the circuit model parameters as follows: $L_{11} = L_A + L_C$, $L_{22} = (L_B + L_C)/N^2$, and $L_{12} = L_{21} = L_C/N$ and the inverse $L_A = L_{11} - NL_{12}$, $L_B = N^2L_{22} - NL_{12}$, and $L_C = NL_{12}$.

It can be seen that – including the turns ratio N – the T model actually has four parameters that can be used to fit the three free parameters of the inductance matrix. One is not constrained to choose N to be the physical turns ratio of the transformer, and sometimes the physical turns ratio is not known. A frequent non-physical choice for N is 1, which results in very simple relationships between the remaining three parameters (the inductances) and the inductance matrix: $L_A = L_{11} - L_{12}$, $L_B = L_{22} - L_{12}$, and $L_C = L_{12}$. Such a model can yield negative inductance values (as long as conservation of energy is obeyed, as noted above) which can actually be useful in circuit design [14].

In the more common case where N is selected as the physical turns ratio of the transformer, the inductances have physical meaning,[1] namely as the primary-side leakage inductance $L_A = L_{l1}$ (representing flux that only couples the primary), the primary-referred magnetizing inductance $L_C = L_{\mu 1}$ (representing flux that couples both windings), and the primary-referred secondary-side leakage inductance $L_B = N^2 L_{l2}$ (representing flux that only couples the secondary; more typically L_B is reflected to the secondary side, forming the secondary-side leakage inductance $L_{l2} = L_B/N^2$).

Turning to the Pi model of the transformer, we can likewise see that there are 4 possible parameters, which can be selectively narrowed to three parameters to realize a necessary and sufficient model for any two-port magnetic component. One way to approach this is to recognize that the Pi model of Fig. 2 can be directly synthesized from the T model by using a Y-Δ transform [15] to convert its inductor network from a T (Y) to an equivalent Pi (Δ) configuration.

The cantilever model of Fig. 2 – so named by its originators because the configuration of the two inductors in the circuit resembles a cantilever [16] – provides exactly the three independent parameters needed to represent a two-port magnetic structure: two inductors (L_G and L_H) and a non-physical turns ratio[2]. The cantilever model can be understood as the T model with one series inductance constrained to be zero or as the Pi model with one shunt inductance constrained to be infinitely large. This model is particularly suitable for use in circuit design, as it makes explicit only two energy storage elements, making its behavior easier to visualize than a model including three inductors. However, since none of

---

[1] Strictly speaking, the above description only applies when flux linking any turn of a given winding links *all* the turns of that winding, such that there is no flux leakage among turns – otherwise it is merely an approximate physical understanding. Flux leakage within a winding is one reason, along with various numerical and measurement issues, that “physical” leakage inductances are sometimes concluded to be negative from experiments.

[2] If the primary or secondary leakage is very small, a cantilever model may be constructed with n approximately equal to the physical turns ratio. In physical windings, however, there is always some leakage flux.

the three parameters has direct physical meaning, it can be difficult to synthesize a magnetic component with the desired parameters.

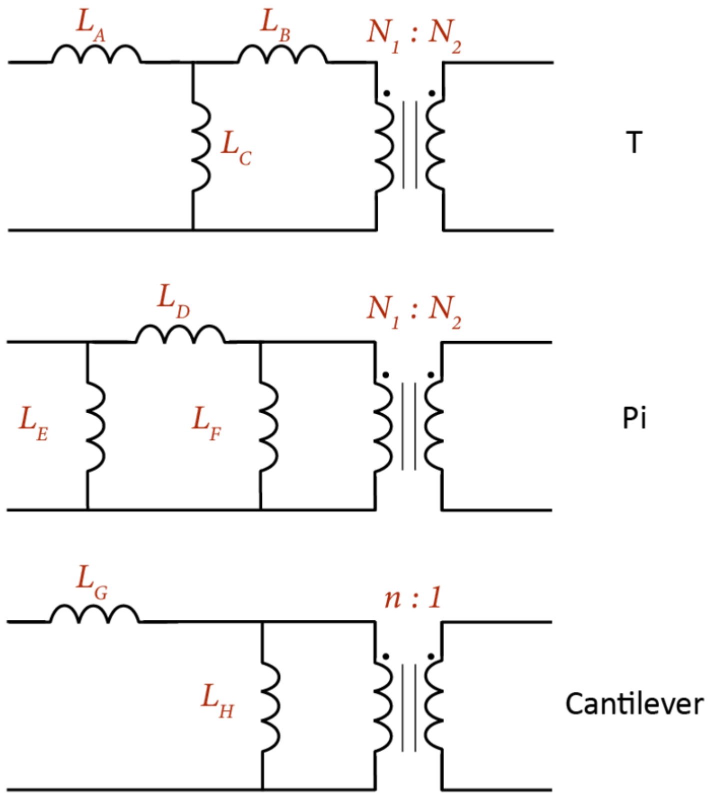

Figure 2 - Three common circuit structures for modeling two-winding transformers. These models can be made mathematically equivalent to each other and to the inductance matrix.

Side box -- Different "types" of transformers

All N-winding magnetic structures based on electromagnetic induction may be modeled in the same way. Nevertheless, it is common to see them referred to by their intended application – flyback transformers, forward transformers, current transformers, Rogowski coils, voltage transformers, common-mode chokes, coupled inductors, sense windings (on inductors), gate-drive transformers, low-/medium-/high-frequency transformers, autotransformers, pulse transformers, variacs, etc. This varied terminology sometimes gives the impression that there is a great variety of physical principles at work, which is not the case. It is important to emphasize that the varied transformer nomenclature refers to a variety of use cases (and hence design goals), not to any distinction in magnetic physics. (While there are electromagnetic components – such as circulators – that incorporate other physical principles, nearly all magnetic components used by power electronics engineers operate based on Faraday's law of electromagnetic induction.) No matter one's choice of terminology, the approaches in this article apply to all such magnetic devices.

For example, a forward transformer is so called because it has been optimized for use in a forward converter, where all of the inductances in the T model are considered parasitic. It is therefore often designed with no core gap and tight coupling between the windings to yield large magnetizing (L_C) and small leakage inductances (L_A, L_B). By contrast, the magnetizing inductance (L_C) in a flyback converter is not parasitic; it plays a direct role in the intended operation of the converter and is expected to store a substantial amount of energy. A flyback transformer is therefore designed with a gap in the core.

Other good examples include instrumentation transformers. A current transformer is typically designed with a single-turn primary and a small resistive burden on the secondary. In this case, the user assumes that nearly all of the primary current flows through the ideal transformer in the T model. A corresponding current flows through the burden resistor to create a sense voltage which is proportional to and in phase with the sensed current. The magnetizing inductance (L_C) and secondary leakage inductance (L_B) are therefore considered parasitic and current transformer designs seek to maximize L_C and minimize L_B. By contrast, a Rogowski coil is also used to sense current, but a well-designed Rogowski coil is meant to be used with a high-impedance secondary load with all of the primary current flowing through the magnetizing inductance (L_C). The magnetizing inductance is not parasitic in this case, and is carefully optimized to create a large signal while inserting a small impedance on the sensed system. Thus, while current transformers are typically designed with high-permeability magnetic cores, Rogowski coils often use no core at all.

Further examples abound, including transformers that intentionally utilize leakage inductance (e.g. in dual-active-bridge converters) and transformers that intentionally use both leakage and magnetizing inductance (e.g. in LLC resonant converters). Nevertheless, the same physics, analysis, characterization, and intuition apply equally well to all cases. Therefore, while there is value in specific nomenclature, it is useful to appreciate the unity of the principles that underly all such magnetic devices and the ability to model them in the same way.

(END OF SIDE BOX)

Indeed, excepting the T model with N chosen as the physical turns ratio, the models of Fig. 2 tend to be more mathematical than physical in how they represent a magnetic component. One can, however, develop circuit models that directly represent the physical flux paths of a magnetic structure. This can be accomplished by forming a magnetic circuit model (including key flux paths and reluctances) and converting it into its corresponding electrical circuit. This process can also be reversed, starting from a desired electrical circuit model of a magnetic component, converting it into an equivalent magnetic circuit, and from there synthesizing a magnetic structure with similar flux paths and reluctances. This procedure is not novel (see e.g. [17,3]), but despite its usefulness the authors rarely see it used and it bears additional emphasis.

To illustrate the physical modeling procedure, we consider an example magnetic structure in Fig. 3. Drawing the relevant flux paths and reluctances yields a magnetic circuit at the top of Fig. 4 with the across variable being MMF (ampere-turns) and the through variable being flux (volt-seconds/turn)[3]. Taking its topological dual yields a circuit with flux as the across variable, MMF as the through variable, and a set of permeances (units Henries, the magnetic analog of conductance). Differentiating the circuit makes the across variable $d\phi/dt$ and through variable $N\ di/dt$, but the relationships represented by the circuit remain true.

Now, we can pass the role of differentiation from the through variable to the permeances, replacing the through variable with NI and the permeances (which enforce the ratio $\mathcal{P} = \frac{across}{through}$) with inductances (which enforce the ratio $L = \frac{across}{d(through)/dt}$). This maintains the exact same constitutive relations between the across and through variables: $d\phi/dt = P\left(N\frac{di}{dt}\right) = \left(L\frac{d}{dt}\right)Ni$. Adding transformers to account for the source turns ratios completes the conversion, with the outer variables becoming electrical volts and amperes. The inner structure is usually reflected to the outside, and the transformers are usually combined – we leave the example in "unfinished" form to highlight the electrical domain coupling into the magnetic domain.

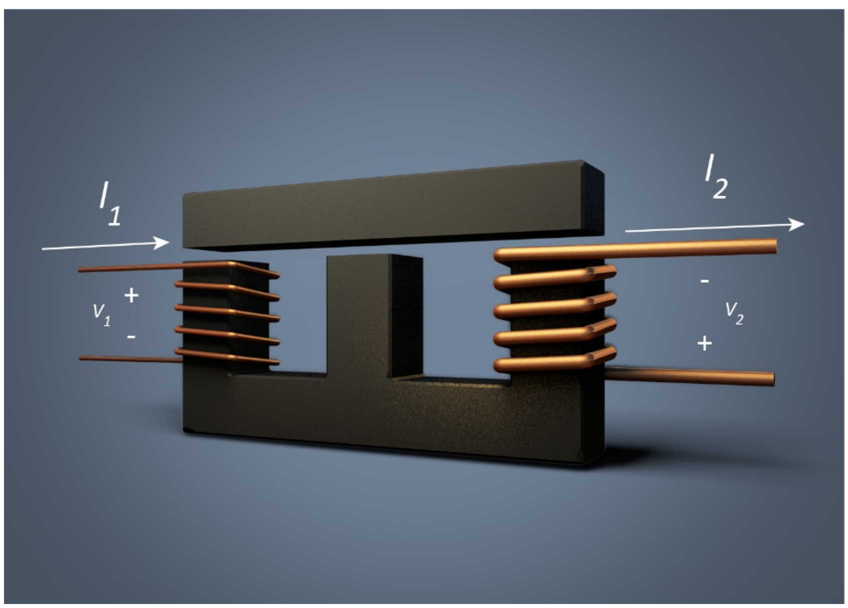

Figure 3 – A two-winding magnetic structure example, used in Fig. 4 to demonstrate the conversion from a magnetic circuit model to an equivalent electric circuit.

---

[3] In the reluctance model, the product of across variable (MMF) and through variable (flux) has units of energy, not power as in electric, mechanical, fluid, or thermal systems. In addition, "dissipation" in the magnetic circuit domain corresponds to energy storage in the electric circuit domain (and, while we do not treat it here, vice versa [18].) This inconsistency with the models of virtually every other physical system is sometimes seen as a theoretical embarrassment of the reluctance model, and more satisfying models have been proposed to replace it [19]. Nevertheless, the reluctance model's ease of use has made it the clear favorite in the field.

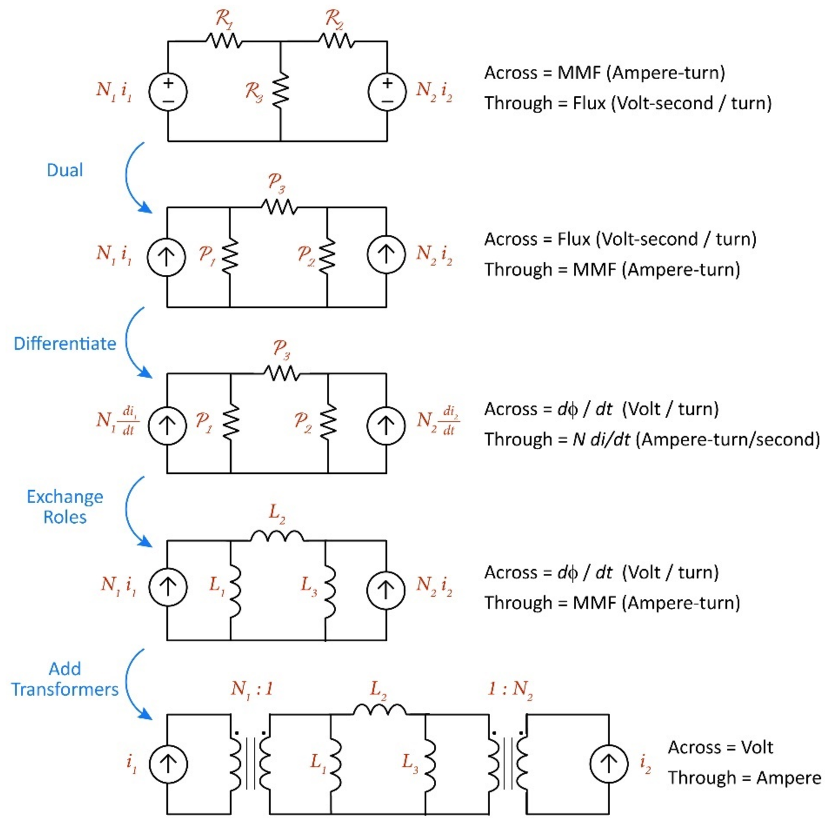

Figure 4 – Magnetic circuits can be converted into electric equivalent circuits through topological duality (and vice versa). This physical modeling approach can be used to analyze existing structures or synthesize a structure with some desired functionality, but it is not guaranteed to have the number of independent parameters required by the inductance matrix.

It can be seen in Fig. 4 that the magnetic circuit and its "direct equivalent" electric circuit are topological duals [17,3]. Thus, these steps can be used to convert between the electric and magnetic domain for the same component. Note that, while we belabor the details for completeness, in practice the transformation is often easily drawn by inspection.

In this example, the physical model reduced to a well-known necessary-and-sufficient representation (the Pi model with a physical turns ratio), but there is no guarantee that it would have. A magnetic circuit can include reluctance paths at many levels of granularity, producing just as many inductances in the electric equivalent circuit. The limit of an ultra-fine-grained reluctance model is similar in essence to a finite-element simulation. A magnetic circuit could also include fewer reluctances than a necessary-and-sufficient model, resulting in a reduced-order electric circuit. Because the identification of *relevant* reluctance paths is an unconstrained choice, the final result may be under- or over-determined (with respect to the $M(M+1)/2$ independent parameters for describing port relationships) and therefore will only match reality to the extent that the original magnetic circuit captures the right amount of information.

Physical modeling of magnetics is most useful in design. If we want some functionality in a circuit, we can reverse the above process to obtain a magnetic circuit and then synthesize an actual component. However, physical models can be less useful in characterizing an existing device, especially for the likely case of an under- or over-defined model. For example, consider the complicated structure of Fig. 5 with many relevant flux paths. With physical modeling, the analysis is straightforward, even considering the flux that links only some turns of each winding (e.g. by modeling each turn as a separate winding, electrically connected in series).[4] However, the 12 reluctances in the model of Fig. 5 is more than the number of parameters in a two-port or even a four-port inductance matrix (three and ten respectively). Therefore, given a prototype of this structure, it is impossible to determine the values of all 12 equivalent circuit inductances by experimentally testing the electrical port behavior, though such tests can determine the values of an inductance matrix or necessary-and-sufficient circuit model. Conversely, if the physical model had too few reluctances/inductors in it to capture the actual flux paths in a practical device, then the resulting circuit model (and any inductance matrix derived from it) would not well represent the behavior of the practical device.

This case shows that the translation between physical and necessary-and-sufficient models can be difficult and the advantages of each approach become more apparent. On paper, physical modeling is the easiest way to understand a structure. Given a physical prototype, experimentally characterizing the component in terms of inductance matrix or necessary-and-sufficient circuit parameters/model is much more straightforward.

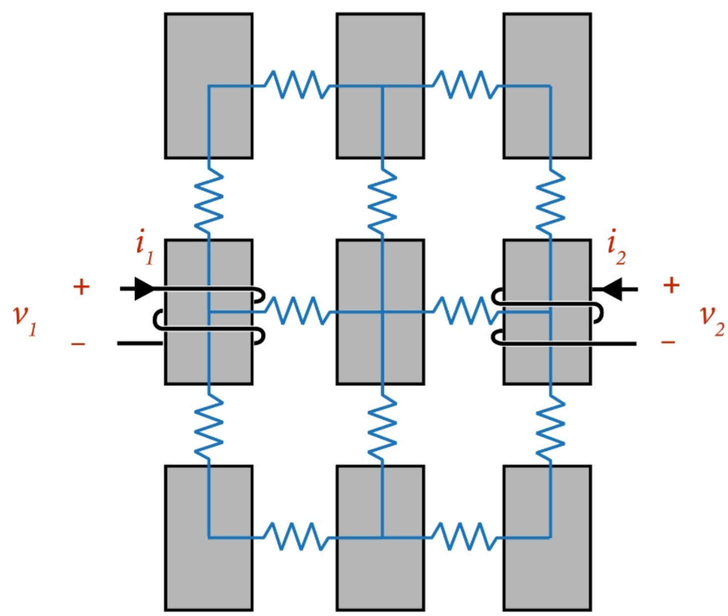

Figure 5 - A bizarre magnetic structure which is difficult to analyze without a many-parameter physical model. While mathematically such a model must reduce to the three independent parameters of the inductance matrix (equivalently, a necessary-and-sufficient circuit model), such a reduction is not always straightforward.

[4] Flux linking only some turns in a winding can be important to model, e.g. to understand the direction and magnitude of B fields within the structure, to capture un-even distribution of voltage on a winding, etc.

Modeling with Three Windings

Moving to three windings changes the modeling landscape substantially. While the mathematical and physical representations extend naturally to M windings, most necessary-and-sufficient circuit representations do not extend so cleanly [20]. The primary exception, and perhaps the most-used of such models is the Extended Cantilever Model [21]. In this model, an M-port magnetic structure is represented by a set of M nodes with an inductance connecting each of them to each other, yielding $M(M-1)/2$ parameters. Each winding couples to one of the M nodes, with the primary having a shunt inductance and a 1:1 turns ratio, and every other turns ratio being an independent variable. This yields M more parameters, for a correct total of $M(M+1)/2$. This model extends naturally to M windings, and any apparent complexity in the model results from the fact that port relationships of magnetic structures simply become quadratically more complicated as a function of M.

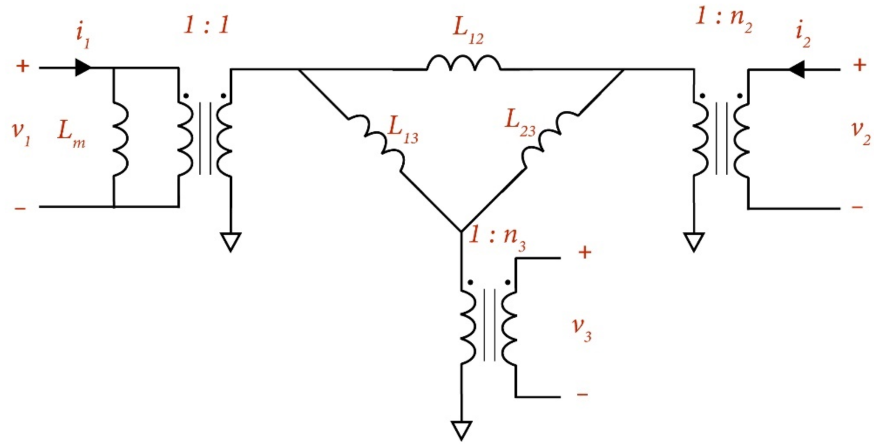

Figure 6 - The Extended Cantilever Model, a necessary-and-sufficient model, for a three-winding structure. This model extends naturally to M ports and $M(M+1)/2$ parameters. Moreover, each parameter can be measured without performing numerically sensitive calculations, though some of the measurements require current sensing which can be challenging at elevated frequencies.

Identifying the $M(M+1)/2$ parameters in any necessary-and-sufficient representation is typically done experimentally, either through experiments on a practical device or through numerical simulations of a model of the device. The recommended measurements for the Extended Cantilever Model are shown in Table 1, with open-circuit measurements used to find the magnetizing inductance and non-physical turns ratios, and short-circuit current measurements used to find the "leakage" inductors. This approach is particularly good since subtractions of measurements are completely avoided, which otherwise could cause small-difference-of-large-numbers problems (which are particularly acute in magnetic systems with very strong or very weak couplings).

Example -- Characterizing a Flyback Transformer (written for presentation in a side box. If not, may want to change transitions)

Measurement difficulties are encountered even in two-winding transformers, and a two-winding example helps demonstrate the challenges. Consider a 5:1 flyback transformer ($N = N_1/N_2 = 5$) with the following measurements (taken from a real transformer):

1) the primary inductance is measured with the secondary open-circuited, yielding $L_{11} = 1987\mu H$;
2) the secondary inductance is measured with the primary open-circuited, yielding $L_{22} = 79.98\mu H$;
3) An ac voltage of 1.047 V is applied to the primary with the secondary open-circuited; the secondary voltage is measured at 0.2082 V.

The T-model transformer parameters are easily found:

$$L_C = NL_{11}\frac{v_2}{v_1} = 1975.6132 \approx 1976\ \mu\text{H}$$
$$L_A = L_{11} - L_C = 1987 - 1975.6132 = 11.3868 \approx 11.39\ \mu\text{H}$$
$$L_B = N^2 L_{22} - L_C = 1999.5 - 1975.6132 = 23.8868 \approx 23.89\ \mu\text{H}$$

In this case, finding L_A and L_B requires subtractions of large numbers that are about 1% apart. Small-percentage errors in the large numbers can yield wildly incorrect results. For example, consider what would happen if the L_{11} and v_2/v_1 measurements each had ± 2% error. First consider L_A, the primary-side leakage inductance. In a flyback converter, this parameter should be known accurately to account for leakage losses or to properly design an active or passive clamp. Calculations of L_A across small measurement errors yield a very wide range of results, as shown in Fig. 7 – an approximately 80 μH range for a nominally 11 μH parameter. Fig. 7 demonstrates that achieving reasonable accuracy of L_A would require the L_{11} measurement to be accurate to ~0.1%, which can be very difficult to achieve.

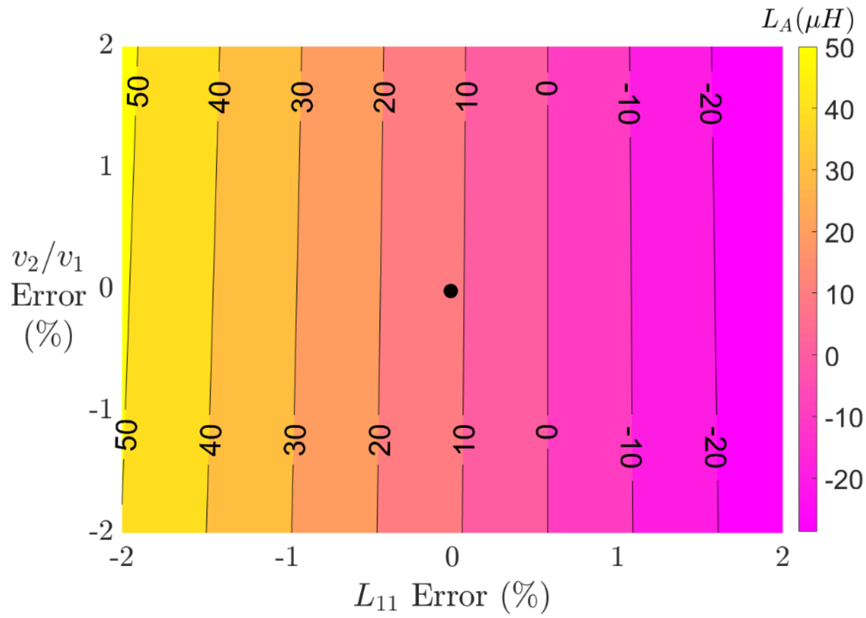

Figure 7 - Calculated values for L_A in the T model of a flyback transformer, showing that small measurement errors can produce a range of results that is ≈ 8 times as large as the nominal result.

The secondary-side leakage is also an important parameter, as it can lead to undesired load regulation and degraded cross-regulation between multiple outputs and/or sense windings (though, as we show, transformers with 3 or more windings have additional complexity beyond simple leakage models). Fig. 8 shows that the primary-referred secondary-side leakage (L_B) is strongly affected by measurement errors of both L_{11} and v_2/v_1 – errors of ±2% of each parameter yield a 160 μH range of results for a nominally 20 μH parameter.

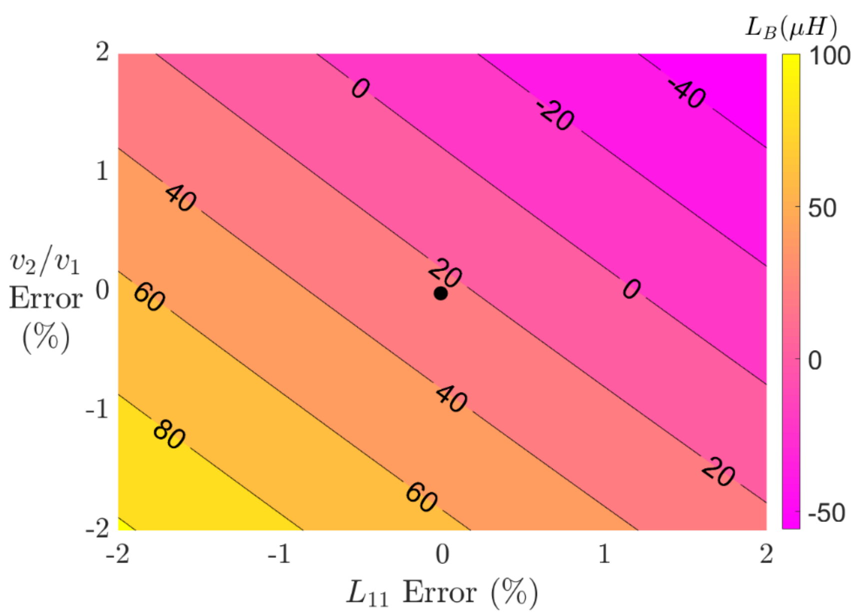

Figure 8 - Calculated values for L_B in the T model of a flyback transformer, showing that small measurement errors in multiple parameters can produce widely varying results

The small-difference-of-large-numbers problem can also yield non-physical results. Calculating the coupling coefficient ($k = L_{12}/\sqrt{L_{11}L_{22}}$) with similar measurement errors yields Fig. 8. The top-right region of Fig. 9 makes clear that small errors are liable to yield a coupling coefficient that is physically impossible ($|k| > 1$).

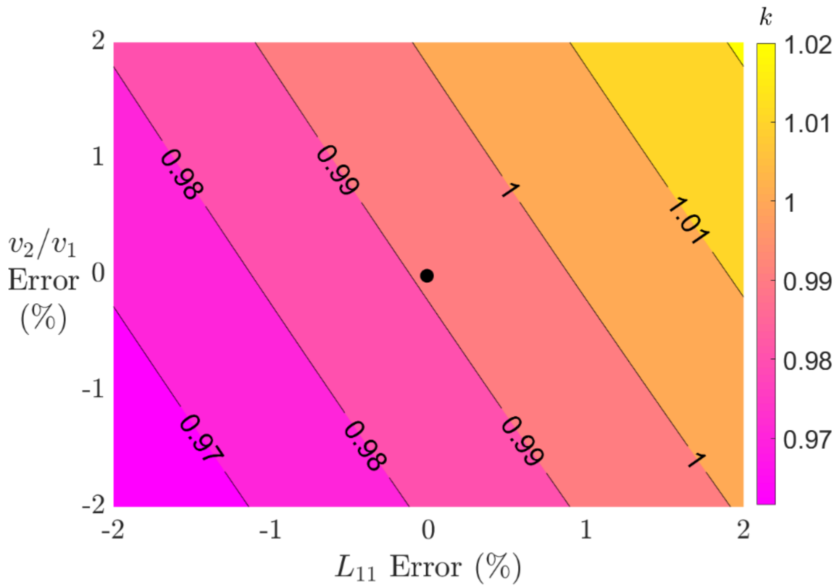

Figure 9 - Calculated values of coupling coefficient for a flyback transformer, showing that small measurement errors can yield non-physical models (e.g. k > 1).

This flyback example highlights the need for modeling approaches with low numerical sensitivity by using only high-accuracy measurements and – where possible – by avoiding subtractions (or at least small differences of large numbers) when computing model parameters.

END OF EXAMPLE

	Apply Condition to Winding				
	1	2	3	Measure	
m_1	v_1	OC	OC	Z_1	$= j\omega L_m$
m_2	v_1	OC	OC	v_2/v_1	$= n_2$
m_3	v_1	OC	OC	v_3/v_1	$= n_3$
m_4	v_1	SC	SC	v_1/i_2	$= j\omega l_{12} \times n_{12}$
m_5	v_1	SC	SC	v_1/i_3	$= j\omega l_{13} \times n_{13}$
m_6	SC	v_2	SC	v_2/i_3	$= j\omega l_{23} \times n_{23}$

Table 1 - Recommended measurements to identify parameters in the Extended Cantilever Model with three windings. These recommendations require short-circuit current measurements but no subtractions. OC means "Open Circuit", SC means "Short Circuit".

As a useful necessary-and-sufficient model, perhaps the only substantive complaint that can be levied against the Extended Cantilever Model is the recommended process for determining model parameters, which includes the need to measure currents at short-circuited ports [22]. Current measurements typically require bulky sensors that themselves impose inductive and/or resistive impedances on the circuit, both of which become more restrictive concerns as frequency increases and size decreases. Given the complexity of the model, it is difficult to predict *a priori* if external impedances, or artificial inductances from measurement loops, will be negligible compared to what one is trying to measure.

Therefore, it would be advantageous to have a necessary-and-sufficient representation that only requires voltage measurements, which are easier to make with high confidence at even tens of MHz. In particular, we would like to use only one-port impedance measurements or two-port voltage ratios that can be obtained on an impedance analyzer. It is also preferable, where possible, to have measurements that require open-circuit terminations rather than short-circuit terminations, as these are easier to realize at high frequency[5]. We would like any required calculations to avoid small-differences-of-large-numbers problems as well.

One way to approach this problem is to observe that the offending measurements in the Extended Cantilever Model arise from the connection of the internal nodes (a delta connection in the three-winding case). We might hypothesize, perhaps without perfect rigor, that creating a model with the graphical dual (i.e. a Y-connection) of the internal section might allow for voltage measurements in place of currents. Such a model is shown in Fig. 10, with available well-behaved measurements in Table 2. Combining these measurements turns out to be fruitful in obtaining every parameter using only one-port impedance and two-port voltage ratio measurements and without any subtractions (Table 3). For completeness, the mappings between this model and the inductance matrix are provided in Table 4; this complements the mappings provided for the cantilever model in [21].

---

[5] At sufficiently high frequencies it becomes difficult to impose sufficiently good short or open circuits at ports; it is partially for this reason that S-parameter measurements become the dominant approach at radio frequencies.

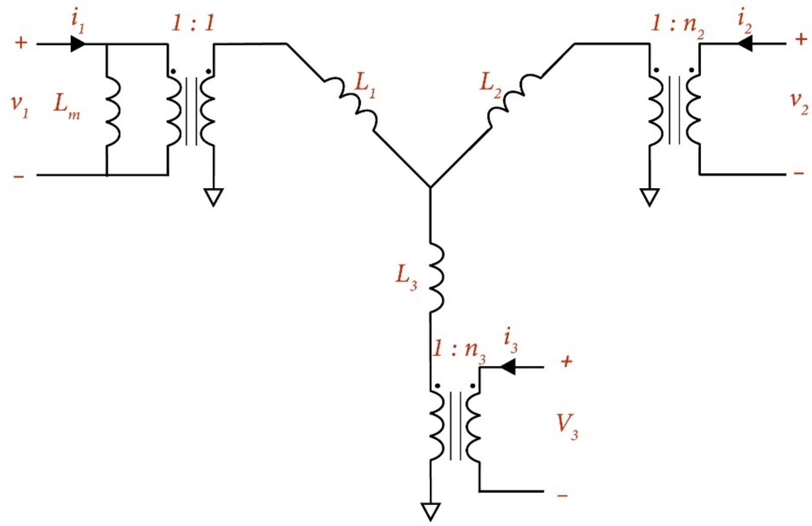

Figure 10 – A modification to the Extended Cantilever Model with the graphical dual of the inner network. For three windings, the designer can characterize each parameter using only one-port impedance and two-port voltage ratio measurements, without any subtractions. It has the same advantages as the Extended Cantilever Model with extended utility at higher frequencies.

	Apply Condition to Winding				
	1	2	3	Measure	
m_1	v_1	OC	OC	$Z_1/j\omega$	$= L_m$
m_2	v_1	OC	OC	v_2/v_1	$= n_2$
m_3	v_1	OC	OC	v_3/v_1	$= n_3$
m_4	v_1	SC	OC	v_3/v_1	$= L_2/(L_2 + L_1) \times n_3$
m_5	v_1	OC	SC	v_2/v_1	$= L_3/(L_3 + L_1) \times n_2$
m_6	SC	v_2	OC	$Z_2/j\omega$	$= (L_2 + L_1) \times n_2^2$
m_7	SC	OC	v_3	$Z_3/j\omega$	$= (L_3 + L_1) \times n_3^2$
m_8	SC	v_2	OC	v_3/v_2	$= L_1/(L_1 + L_2) \times n_3/n_2$
m_9	SC	OC	v_3	v_2/v_3	$= L_1/(L_1 + L_3) \times n_2/n_3$

Table 2 - Well-behaved measurements available for the three-winding model in Fig. 9.

L_m	m_1
n_2	m_2
n_3	m_3
L_1	$m_8 m_6/(m_2 m_3)$ OR $m_9 m_7/(m_2 m_3)$
L_2	$m_4 m_6/(m_3 m_2^2)$
L_3	$m_5 m_7/(m_2 m_3^2)$

Table 3 - Measurements from Table 2 can be combined to yield the model parameters in Fig. 9 without resorting to subtractions and the ensuing numerical dangers.

We have therefore achieved a necessary-and-sufficient circuit model that can represent three-winding structures and can be characterized by measurements that are well-behaved to high frequency, making such a model very suitable for many power electronics applications.

$L_{11} =$	L_m	$L_m =$	L_{11}
$L_{22} =$	$(L_m + L_1 + L_2) \times n_2^2$	$n_2 =$	L_{12}/L_{11}
$L_{33} =$	$(L_m + L_1 + L_3) \times n_3^2$	$n_3 =$	L_{13}/L_{11}
$L_{12} =$	$L_m \times n_2$	$L_1 =$	$L_{23}L_{11}^2/(L_{12}L_{13}) - L_{11}$
$L_{13} =$	$L_m \times n_3$	$L_2 =$	$L_{22}L_{11}^2/L_{12}^2 - L_{23}L_{11}^2/(L_{12}L_{13})$
$L_{23} =$	$(L_m + L_1) \times n_2 n_3$	$L_3 =$	$L_{33}L_{11}^2/L_{13}^2 - L_{23}L_{11}^2/(L_{12}L_{13})$

Table 4 - Mapping the model in Fig. 9 to the inductance matrix and back.

Before extending the model to >3 windings, it is useful to note the variety of applications of three-winding transformers. Many applications have dual input or dual output (especially, for example, supplying "hotel" or auxiliary power to the analog and digital functions within a power converter). Transformers in high-frequency power conversion commonly contain an auxiliary winding for sensing. Recent research has also made greater use of stacking power conversion units in multiple voltage domains and using dual-input transformers to recombine the power and provide isolation [5-8]. Additionally, center-tapped secondaries and novel approaches to circuit-magnetics interaction like that of [23] are structures that, for purposes of modeling, are 3-winding structures. Furthermore, the use of "integrated magnetics" can achieve both high density and functional integration.

Extension to >3 Windings

A strong benefit of the Extended Cantilever Model is that it can, in principle, model general *M*-winding magnetic components. Insofar as the proposed model involves a graphical dual of (part of) the Extended Cantilever Model, it is likewise extensible to any number of windings. However, for more than three windings, the Extended Cantilever Model has a non-planar graph, i.e. there are branches that cross each other, and there is no way to draw the circuit without the crossings. Taking the dual of a non-planar graph is ordinarily impossible, but can be enabled with a small circuit trick as demonstrated in Fig. 11 [24]. Any crossing branches may be redrawn as intersecting, provided that an ideal 1:1 transformer is inserted on one of the branches. Thus the voltage in one branch still has no effect on the other branch, just as when they were disconnected. Once this modified planar (but electrically equivalent) graph has been drawn, the dual may be taken as usual.

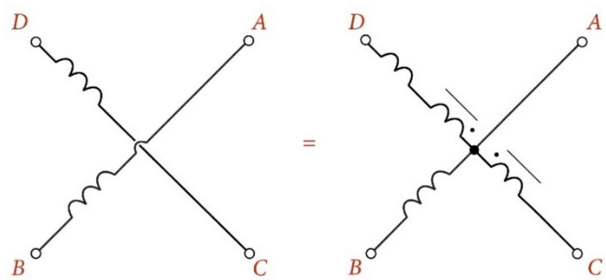

Figure 11 - Topological duality is not directly applicable to non-planar graphs. When unavoidable crossings occur, the graph may be modified to an electrical equivalent which is graphically planar [24] and the dual may be found [13].

Performing these operations for the four-winding case converts the Extended Cantilever Model (Fig. 12) to the proposed model (Fig 13). As before, a table of well-behaved measurements for the proposed model is shown in Table 5.

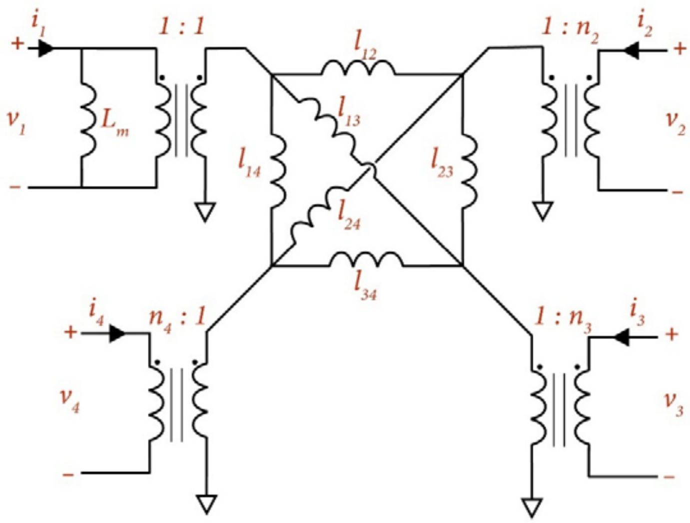

Figure 12 - The Extended Cantilever Model for four windings contains one unavoidable non-planar crossing. The dual of the inner section may be taken using the method in Fig. 10.

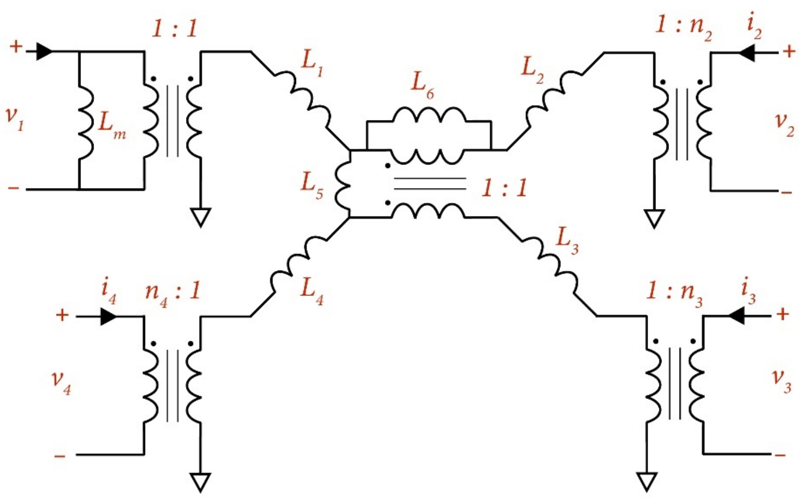

Figure 13 - Four-winding version of the proposed model, as derived from the Extended Cantilever Model. In this case, most parameters may still be obtained using only one-port impedance and two-port voltage ratio measurements. Some parameters may require current sensing or subtractions to determine, though several options are available to choose from to minimize error.

	Apply Condition to Winding					
	1	2	3	4	Measure	
m_1	v_1	OC	OC	OC	Z_1	$= j\omega L_m$
m_2	v_1	OC	OC	OC	v_2/v_1	$= n_2$
m_3	v_1	OC	OC	OC	v_3/v_1	$= n_3$
m_4	v_1	OC	OC	OC	v_4/v_1	$= n_4$
m_5	v_1	OC	OC	SC	v_2/v_1	$= (L_4 + L_5)/(L_1 + L_4 + L_5) \times n_2$
m_6	v_1	OC	OC	SC	v_3/v_1	$= L_4/(L_1 + L_4 + L_5) \times n_3$
m_7	v_1	OC	SC	OC	v_2/v_1	$= (L_3 + L_5)/(L_1 + L_3 + L_5 + L_6) \times n_2$
m_8	v_1	OC	SC	OC	v_4/v_1	$= (L_3 + L_6)/(L_1 + L_3 + L_5 + L_6) \times n_4$
m_9	v_1	SC	OC	OC	v_3/v_1	$= L_2/(L_1 + L_2 + L_6) \times n_3$
m_{10}	v_1	SC	OC	OC	v_4/v_1	$= (L_2 + L_6)/(L_1 + L_2 + L_6) \times n_4$
m_{11}	SC	v_2	OC	OC	Z_2	$= j\omega(L_1 + L_2 + L_6) \times n_2^2$
m_{12}	SC	OC	v_3	OC	Z_3	$= j\omega(L_1 + L_3 + L_5 + L_6) \times n_3^2$
m_{13}	SC	OC	OC	v_4	Z_4	$= j\omega(L_1 + L_4 + L_5) \times n_4^2$
m_{14}	SC	v_2	OC	OC	v_3/v_2	$= (L_1 + L_6)/(L_1 + L_2 + L_6) \times n_3/n_2$
m_{15}	SC	v_2	OC	OC	v_4/v_2	$= L_1/(L_1 + L_2 + L_6) \times n_4/n_2$
m_{16}	SC	OC	v_3	OC	v_2/v_3	$= (L_1 + L_6)/(L_1 + L_3 + L_5 + L_6) \times n_2/n_3$
m_{17}	SC	OC	v_3	OC	v_4/v_3	$= (L_1 + L_5)/(L_1 + L_3 + L_5 + L_6) \times n_4/n_3$
m_{18}	SC	OC	OC	v_4	v_2/v_4	$= L_1/(L_1 + L_4 + L_5) \times n_2/n_4$
m_{19}	SC	OC	OC	v_4	v_3/v_4	$= (L_1 + L_5)/(L_1 + L_4 + L_5) \times n_3/n_4$

Table 5 - Available well-behaved measurements for the proposed model, extended to four windings in Fig. 12. While some of the measurements require short-circuit terminations at ports, none of the tests here require current sensing.

In Table 6, we find that the proposed model for four-winding structures can yield 7/10 parameters with fully well-behaved measurements and calculations (more than the 4/10 such parameters of the Extended Cantilever Model). The remaining three parameters may be obtained by less desirable means (subtraction, current sensing, etc.) where sensitivity allows, and there are several ways to obtain each of the remaining parameters.

L_m	m_1
n_2	m_2
n_3	m_3
n_4	m_4
L_1	$m_{18}m_{13}/(m_2m_4)$ OR $m_{15}m_{11}/(m_2m_4)$
L_2	$m_9m_{11}/(m_3m_2^2)$
L_3	-
L_4	$m_6m_{13}/(m_3m_4^2)$
L_5	-
L_6	-

Table 6 - Well-behaved measurements for the proposed four-winding model can be used to derive seven of the ten model parameters without subtraction, an improvement over 4/10 for the four-winding Extended Cantilever Model.

Conclusion

As designers strive to best take advantage of good switching devices and best grapple with the magnetic bottleneck, the solution often involves more complex magnetic structures. Modeling such structures with mathematics, necessary-and-sufficient circuit models, and physical circuit models is an essential element in understanding their complicated behavior. Our brief review here has covered some of the primary modeling approaches, their advantages and disadvantages, and the translation between them.

In addition, we introduced a necessary-and-sufficient circuit model with characterization advantages over the Extended Cantilever Model. In a three-winding structure, the complete set of parameters can be obtained with only one-port impedance and two-port voltage ratio measurements, which can reliably be obtained to very high frequencies (compared to 3/6 parameters in the Extended Cantilever Model). In a four-winding structure, the proposed model can find 7/10 parameters in this way (compared to 4/10 for the Extended Cantilever Model). This model may therefore be useful for a wide range of many-winding magnetic structures, with a high ceiling on appropriate frequencies.

Authors

Alex Hanson (ajhanson@utexas.edu)
Alex J. Hanson (S’14, M’19) received the B.E. degree from Dartmouth College in 2014 and the S.M. and Ph.D. degrees from the Massachusetts Institute of Technology in 2016 and 2019 respectively. In 2019, he joined the University of Texas at Austin as an assistant professor. His research interests include high-frequency circuits and magnetics for energy conversion. He is a Member of the IEEE.

David Perreault (djperrea@mit.edu)
David J. Perreault (S’91, M’97, SM ’06, F’13) received the B.S. degree from Boston University, Boston, MA, and the S.M. and Ph.D. degrees from the Massachusetts Institute of Technology, Cambridge, MA. In 1997 he joined the MIT Laboratory for Electromagnetic and Electronic Systems as a Postdoctoral Associate, and became a Research Scientist in the laboratory in 1999. In 2001, he joined the MIT Department of Electrical Engineering and Computer Science, where he is presently the Joseph F. and Nancy P. Keithley Professor of Electrical Engineering and Computer Science. He has held multiple roles within the EECS department, most recently as Associate Department Head from November 2013 – December 2016. His research interests include design, manufacturing, and control techniques for power electronic systems and components, and in their use in a wide range of applications. He also consults in industry, and co-founded Eta Devices, inc. (acquired by Nokia in 2016) and Eta Wireless, inc., startup companies focusing on high-efficiency RF power amplifiers. Dr. Perreault received the Richard M. Bass Outstanding Young Power Electronics Engineer Award, the R. David Middlebrook Achievement Award, the ONR Young Investigator Award, and the SAE Ralph R. Teetor Educational Award, and is co-author of twelve IEEE prize papers.

References

[1] C. R. Sullivan, B. A. Reese, A. L. F. Stein and P. A. Kyaw, "On size and magnetics: Why small efficient power inductors are rare," *2016 International Symposium on 3D Power Electronics Integration and Manufacturing (3D-PEIM)*, Raleigh, NC, 2016, pp. 1-23.

[2] C. Sullivan, private communication, Jul. 2019. Dr. Sullivan credits J. Popovic and D. Maksimovic with the origin of the imagery.

[3] Severns, R. and Bloom, G. (1985). *Modern DC-to-DC Switchmode Power Converter Circuits*. 1st ed. New York: Van Nostrand Reinhold Company, Inc.

[4] S. Biswas, "Application of Integrated Magnetics and Discontinuous Conduction Mode to Multi-Port DC-DC Power Conversion for Integrating PV Panels with Storage," PhD Thesis, University of Minnesota, USA, 2016.

[5] J. A. Santiago-Gonzalez, D. M. Otten, S. Lim, K. K. Afridi and D. J. Perreault, "Single phase universal input PFC converter operating at HF," *2018 IEEE Applied Power Electronics Conference and Exposition (APEC)*, San Antonio, TX, 2018, pp. 2062-2069.

[6] R. A. Abramson, S. J. Gunter, D. M. Otten, K. K. Afridi and D. J. Perreault, "Design and Evaluation of a Reconfigurable Stacked Active Bridge DC–DC Converter for Efficient Wide Load Range Operation," in *IEEE Transactions on Power Electronics*, vol. 33, no. 12, pp. 10428-10448, Dec. 2018.

[7] M. Chen, K. K. Afridi, S. Chakraborty and D. J. Perreault, "Multitrack Power Conversion Architecture," in *IEEE Transactions on Power Electronics*, vol. 32, no. 1, pp. 325-340, Jan. 2017.

[8] S. J. Gunter, K. K. Afridi, D. M. Otten, R. A. Abramson and D. J. Perreault, "Impedance control network resonant step-down DC-DC converter architecture," *2015 IEEE Energy Conversion Congress and Exposition (ECCE)*, Montreal, QC, 2015, pp. 539-547.

[9] L.F. Casey, A.F. Goldberg, and M.F. Schlecht, "Issues Regarding the Capacitance of 1-10 MHz Transformers," *1988 IEEE Applied Power Electronics Conference,* pp. 352-359.

[10] W.G. Hurley, E. Gath, and J.G. Breslin, "Optimizing the AC Resistance of Multilayer Transformer Windings with Arbitrary Current Waveforms," *IEEE Trans. Power Electronics*, Vol. 15, No. 2, March 2000, pp. 369-376.

[11] M. Chen, M. Araghchini, K.K. Afridi, J.H. Lang and D.J. Perreault, "A Systematic Approach to Modeling Impedances and Current Distribution in Planar Magnetics", *IEEE Transactions on Power Electronics*, Vol. 31, No. 1, pp. 560-580, January 2016.

[12] K. Venkatachalam, C.R. Sullivan, T. Abdallah, and H. Tacca, "Accurate Prediction of Ferrite Core Loss with Nonsinusoidal Waveforms using only Steinmetz Parameters," *2002 IEEE Workshop on Computers in Power Electronics,* 2002, pp. 36-41.

[13] Desoer, C. and Kuh, E. (1966). *Basic Circuit Theory*. 1st ed. New York: McGraw-Hill Education.

[14] T.C. Neugebauer, J.W. Phinney, and D.J. Perreault, "Filters and Components with Inductance Cancellation," *IEEE Transactions on Industry Applications*, Vol. 40, No. 2, pp. 483-490, March/April 2004.

[15] A.E. Kennelly, "Equivalence of triangles and three-pointed stars in conducting networks", *Electrical World and Engineer*, vol. 34, pp. 413–414, 1899.

[16] D. Maksimovic, private communication, March 2019.

[17] E.C. Cherry, “The duality between interlinked electric and magnetic circuits and the formation of transformer equivalent circuits,” *Proceedings of the Physical Society,* Section B, 1949, Vol. 62, No. 2, p. 101-111.

[18] E.R. Laithwaite, “Magnetic Equivalent Circuits for Electrical Machines,” *Proc. IEE*, Vol. 114, No. 11, Nov. 1967.

[19] D. C. Hamill, "Lumped equivalent circuits of magnetic components: the gyrator-capacitor approach," in *IEEE Transactions on Power Electronics*, vol. 8, no. 2, pp. 97-103, April 1993.

[20] J. G. Hayes, N. O'Donovan and M. G. Egan, "The extended T model of the multiwinding transformer," *2004 IEEE 35th Annual Power Electronics Specialists Conference (IEEE Cat. No.04CH37551)*, Aachen, Germany, 2004, pp. 1812-1817 Vol.3.

[21] R. W. Erickson and D. Maksimovic, "A multiple-winding magnetics model having directly measurable parameters," *PESC 98 Record. 29th Annual IEEE Power Electronics Specialists Conference (Cat. No.98CH36196)*, Fukuoka, 1998, pp. 1472-1478 vol.2.

[22] M. Shah and K. D. T. Ngo, "Parameter extraction for the extended cantilever model of magnetic component windings," in *IEEE Transactions on Aerospace and Electronic Systems*, vol. 36, no. 1, pp. 260-266, Jan. 2000.

[23] M. K. Ranjram, I. Moon and D. J. Perreault, "Variable-Inverter-Rectifier-Transformer: A Hybrid Electronic and Magnetic Structure Enabling Adjustable High Step-Down Conversion Ratios," in *IEEE Transactions on Power Electronics*, vol. 33, no. 8, pp. 6509-6525, Aug. 2018.

[24] A. Bloch, “On Methods for the Construction of Networks Dual to Non-Planar Networks,” in Proc. Phys. Soc., vol. 58, pp. 677-694, Jun. 1946.